Periodic Mesoporous Ionosilica Nanoparticles for BODIPY Delivery and Photochemical Internalization of siRNA

Braham Mezghrani, Lamiaa Ali, Sara Jakimoska, Frédérique Cunin, Peter Hesemann, Jean-Olivier Durand, Nadir Bettache

ChemPlusChem

Research Article
doi.org/10.1002/cplu.202300021

Chemistry Europe
European Chemical Societies Publishing

www.chempluschem.org

Special Collection

Periodic Mesoporous Ionosilica Nanoparticles for BODIPY Delivery and Photochemical Internalization of siRNA

Braham Mezghrani,[a, b] Lamiaa M. A. Ali,[a, c] Sara Jakimoska,[a] Frédérique Cunin,[b] Peter Hesemann,[b] Jean-Olivier Durand,[b] and Nadir Bettache*[a]

Periodic Mesoporous Ionosilica Nanoparticles (PMINPs) made *via* co-condensation reactions starting from an ionosilica precursor and a porphyrin derivative were used for simultaneous BODIPY/siRNA delivery in cancer cells. We observed high BODIPY loading capacities and efficiencies of the PMINPs that are triggered by anion exchange. siRNA adsorption took place on the surface of the nanoparticles, whereas BODIPY was encapsulated within the core of the nanoparticles. BODIPY release was found to be pH-dependent. Our results indicate 94% BODIPY release after 16 h at pH 4, whereas only 2% were released at pH 7.4. Furthermore, complexation with siRNA against luciferase gene was observed at the surface of PMINPs and gene silencing through its delivery *via* photochemical internalization (PCI) mechanism was efficient in MDA-MB-231 breast cancer cells expressing stable luciferase.

Introduction

Periodic Mesoporous Ionosilica Nanoparticles (PMINPs) are a new and particularly versatile class of silica based nanoparticles. PMINPs are related to Mesoporous Organosilica Nanoparticles (MONPs), which have been particularly studied for biological applications.[1] PMINPs are prepared exclusively from cationic organosilane precursors without any silica source.[2] As a consequence, the resulting nanoparticles contain a very high number of immobilized ionic groups that significantly modify the physico-chemical properties. As examples, PMINPs show high hydrophilicity[3] and remarkable anion exchange properties. They efficiently adsorb anionic drugs such as diclofenac[2] and gemcitabine monophosphate *via* anion exchange processes.[4] PMINPs also efficiently bind polynucleotides such as siRNA *via* electrostatic interactions between the negatively charged biopolymer and the positive charges that are localized on the surface of the nanoparticles.[5] Finally, photochemical properties were conferred to PMINPs through the incorporation of a photosensitizer. We recently reported PMINPs containing covalently bound porphyrin groups. These nano-objects were successfully used for photodynamic therapy and photochemical internalization of siRNA.

In this work, we focused on the simultaneous delivery of two anionic compounds of different size (small molecule *vs* macromolecule), namely BODIPY and siRNA, promoted by porphyrin doped PMINPs. We used BODIPY as a fluorescent model compound for anionic drugs for its ease detection.

The BODIPY molecule used in this study (Figure 1) contains a carboxylic acid function that allows the generation of an anionic carboxylate *via* deprotonation. Its uptake and release can easily be monitored with UV-Vis spectroscopy. Further, it is a small molecule that was easily encapsulated in the pores of the PMINPs, whereas siRNA was adsorbed on the surface of the nanoparticles. Herein, we studied photochemical release of siRNA through a photochemical internalization (PCI) mechanism, and BODIPY was successfully released in the cytoplasm of cancer cells. PMINPs therefore appear as universal and multifunctional transport vehicles for various anionic species. The transport mechanism can be controlled both *via* the size of the adsorbents and the texture of the nanoparticles together with the acidity/basicity of the adsorbents.

[a] Dr. B. Mezghrani, Dr. L. M. A. Ali, S. Jakimoska, Dr. N. Bettache
IBMM, Univ. Montpellier-CNRS-ENSCM
1919, route de Mende
34293 Montpellier Cedex 05 (France)
E-mail: nadir.bettache@umontpellier.fr
[b] Dr. B. Mezghrani, Dr. F. Cunin, Dr. P. Hesemann, Dr. J.-O. Durand
ICGM, Univ. Montpellier-CNRS-ENSCM
1919, route de Mende
34293 Montpellier Cedex 05 (France)
[c] Dr. L. M. A. Ali
Department of Biochemistry
Medical Research Institute
Alexandria University
Alexandria (Egypt)

Special Collection Part of a Special Collection on Photodynamic Therapy

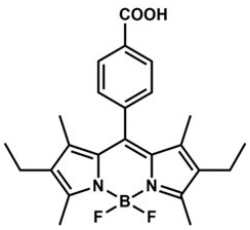

Figure 1. Chemical structure of the used BODIPY derivative.

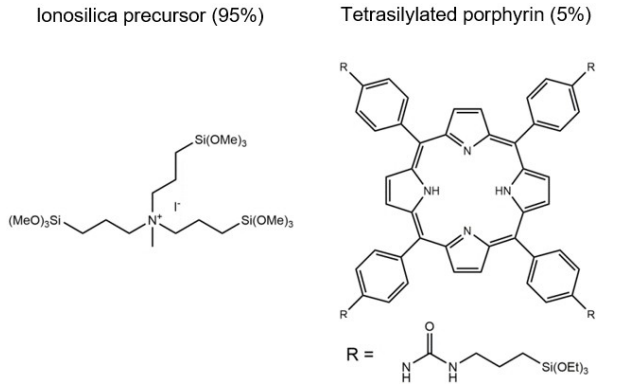

Figure 2. Silylated precursors used for the synthesis of the nanoparticles.

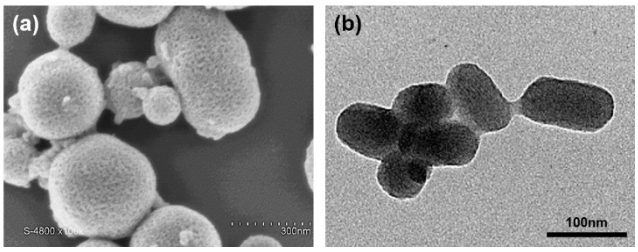

Figure 3. Scanning electron microscopy (a) and transmission electron microscopy (b) images of PMINPs at 200 μg.mL $^{-1}$.

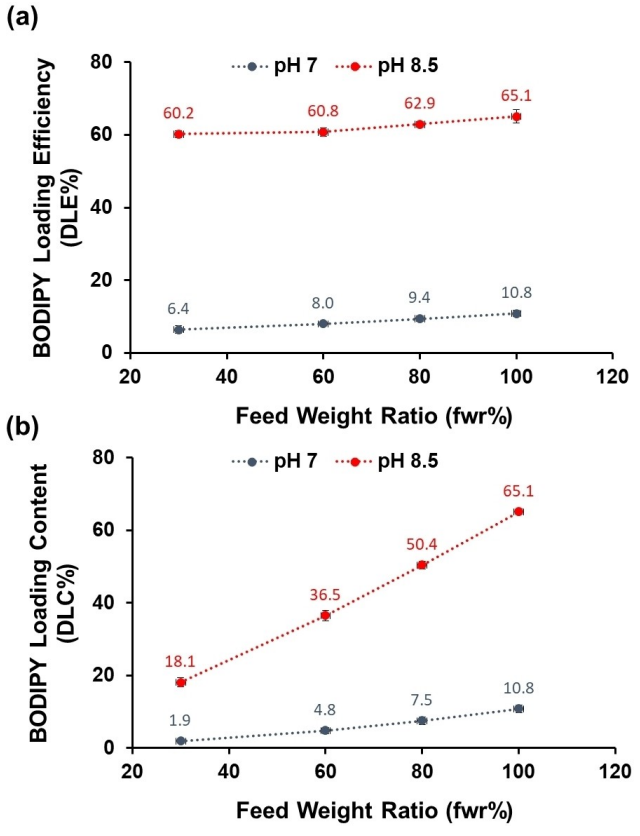

Figure 4. Encapsulation of BODIPY. (a) Loading efficiencies and (b) capacities of PMINPs at pH 7 (blue curves) and 8.5 (red curves).

Results and Discussion

PMINPs were synthesized according to our previous publication[5] from the cationic ionosilica precursor and tetrasilylated porphyrin (Figure 2) in a molar ratio of 95:5. We chose a large excess of the ionosilica precursor in order to guarantee that the porphyrin photosensitizer is incorporated within an ionosilica matrix and to ensure the hydrophilic character of the formed nanoparticles.

We used sodium hexadecylsulfate (SHS) as porogen that generates mesoporosity and triethylbenzene (TEB) that allows increasing the pore diameter, together with nonionic surfactant F127 and silylated PEG2000 in order to limit nanoparticle growth and aggregation. In this way, highly porous PMINPs (S_{BET} = 1015 $m^2 g^{-1}$) with large pore diameter (D = 5.1 nm) were obtained *via* a hydrolytic sol-gel procedure. SEM and TEM characterizations shown in Figure 3 indicated the formation of porous ionosilica nanorods of 108 ± 9 nm length and 54 ± 4 nm width (TEM). Dynamic light scattering (DLS) attested the presence of nanoparticles displaying a diameter of 140 ± 23 nm, with PDI of 0.18. By adding a tetrasilylated porphyrin covalently trapped inside the walls of the material, PCI of siRNA was successfully carried out with green light excitation.[5]

First, we studied the adsorption of BODIPY (Figure 1) using the PMINPs. Buffer solutions (pH 7 and 8.5) were used and feed weight ratios (fwr) from 30 to 100% were investigated (Figure 4).

The drug loading efficiencies (DLE, Figure 4a) were very low at pH 7 and did not exceed 11%, whereas much higher results were obtained for pH 8.5 with a maximum value of 65% at fwr 100%. The drug loading capacities (DLC, Figure 4b) reached maximum values of 65% at fwr 100% at pH 8.5. Once more, much lower values were obtained at pH 7. The pH dependent drug encapsulation suggests that BODIPY is deprotonated at pH 8.5 and strongly interacts with the cationic ammonium centers within the PMINPs, resulting in efficient BODIPY adsorption *via* anion exchange. In order to confirm these results, we monitored the BODIPY adsorption on the PMINPs *via* UV-Vis spectroscopy (Figure 5).

The PMINPs showed characteristic signal of porphyrin derivatives (Soret band) at 433 nm and BODIPY in solution showed a characteristic absorption at 524 nm (Figure 5a). When the encapsulation was performed at pH 7, BODIPY could not be detected in PMINPs (Figure 5b), whereas a strong BODIPY absorption band was observed at 524 nm when the adsorption process was carried out at pH 8.5. These results are in nice agreement with high drug loading efficiencies and capacities previously observed under these conditions (Figure 4). Fluorescence spectroscopy was performed (Figure 5c) and the spectra confirm that PMINPs and PMINPs@BODIPY have the same behavior after an excitation at 430 nm. We also carried out Zeta potential measurements with PMINPs before and after BODIPY adsorption. We observed that the zeta potential of the PMINPs slightly diminishes after BODIPY loading, pointing a high number of surface located positive charges in all systems (Table 1). This result also gives a strong indication that BODIPY was mainly loaded in the pores of the material.

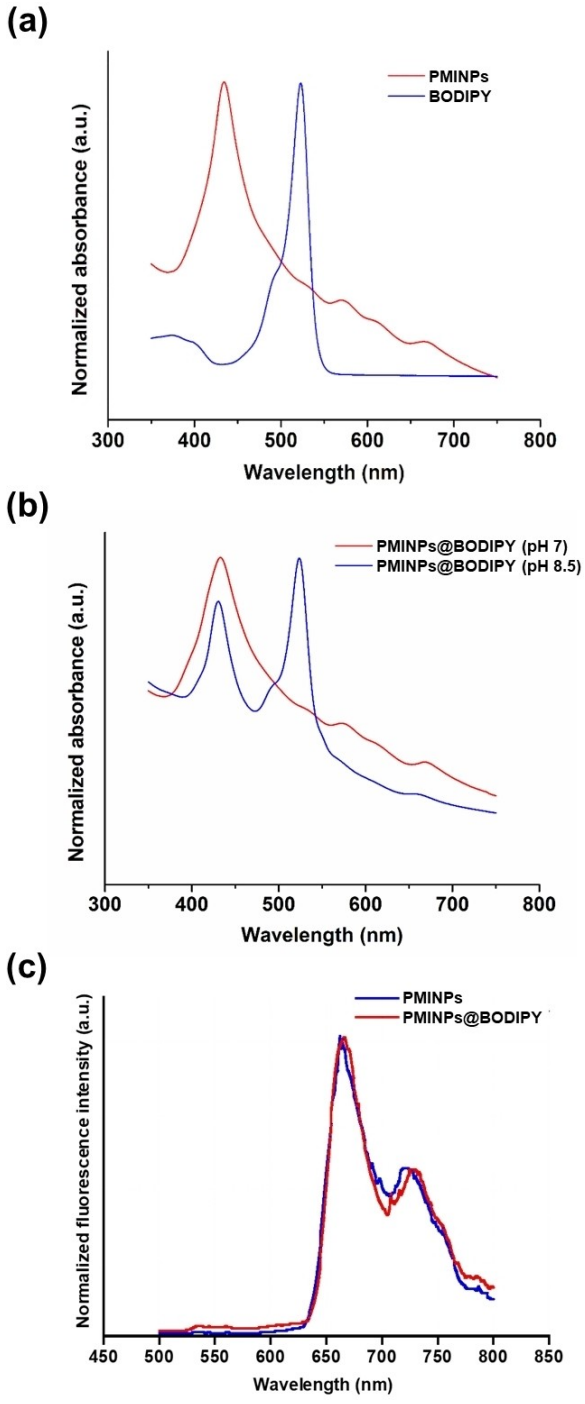

Figure 5. Spectroscopic characterizations. (a) UV-Vis spectra of free PMINPs (red curve) and free BODIPY (blue curve) (b) UV-Vis spectra of PMINPs@BODIPY recovered after BODIPY loading at pH 7 (red curve) and pH 8.5 (blue curve) (c) Fluorescence spectra (λ_{exc} = 430 nm) of PMINPs (blue curve) and PMINPs@BODIPY (red curve).

According to the BODIPY Loading Content value we obtained, our nano-system (PMINPs) demonstrated an important ability to encapsulate BODIPY (loading rate ≤ 65 %).

PMINPs were compared to other delivery nano-systems reported in the literature, and the results are summarized in Table 2. The nanoparticles reported here appeared as efficient as other systems previously reported in the literature.

Table 1. Results of Zeta Potential measurements carried out on PMINPs@-BODIPY at a concentration of 200 µg.mL^{-1} in water.

Compound	Zeta ± SD [mV]
PMINPs	+35.8 ± 0.52
PMINPs@BODIPY **fwr** = **30 %**	+25.7 ± 1.23
PMINPs@BODIPY **fwr** = **60 %**	+28.1 ± 1.34
PMINPs@BODIPY **fwr** = **80 %**	+30.5 ± 0.45
PMINPs@BODIPY **fwr** = **100 %**	+31.2 ± 1.21

After having ascertained the efficient BODIPY adsorption by PMINPs at slightly basic pH, we studied in a second time its release, once more as a function of pH (Figure 6).

At pH 7.4, we observed almost no BODIPY release after 24 h incubation. This result can be explained by strong ionic interactions between the anionic carboxylate groups of BODIPY and the cationic ammonium groups of the PMINPs scaffold. When incubated at pH 4, a significant BODIPY release was

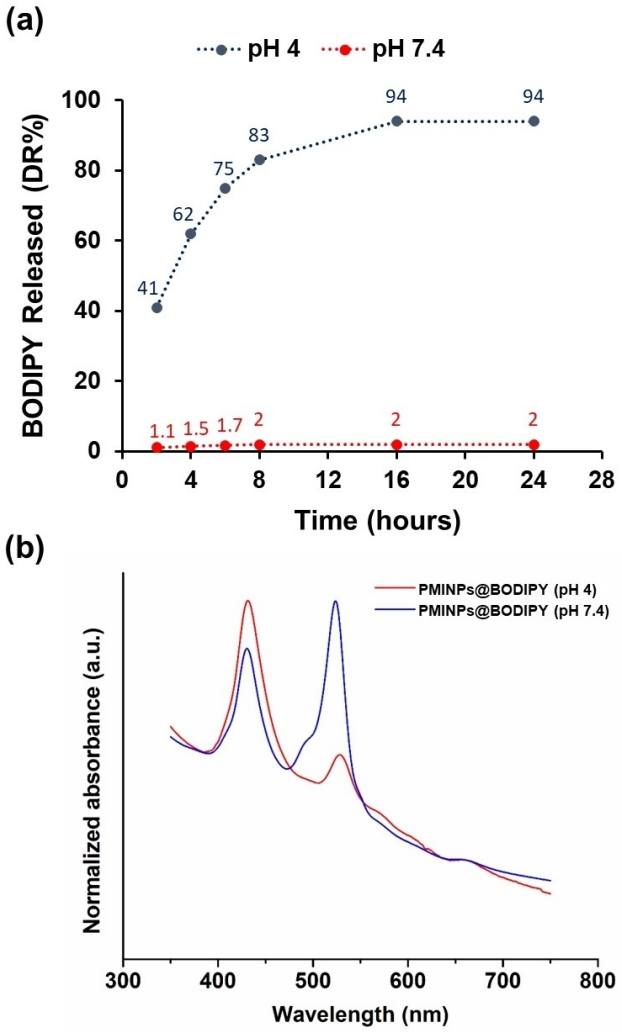

Figure 6. BODIPY release from PMINPs. (a) BODIPY release at pH 4 and pH 7.4 and the calculation of percentage of drug released (b) UV-Vis spectra recorded at the end of BODIPY release process at pH 4 and pH 7.4.

Table 2. Comparison of the Drug Loading Content rates of various nanoparticular vehicles.

Nature of nano-system	Encapsulation mechanism	DLC [%]	Ref.
PMINPs	Non-covalent electrostatic interactions, π-stacking, hydrogen bonds or hydrophobic interactions	≤65%	this work
Mesoporous silica NPs		≤69%	[6]
Mesoporous carbon NPs		≤59%	[7]
Organometallic NPs	Coordination bonds, π-stacking or hydrophobic interactions	≤58%	[8]
Protein NPs	Covalent bonds with the protein matrix, π-stacking, hydrophobic interactions or crystallization	≤44%	[9]
Polymer NPs	Covalent bonds	≤58%	[10]
Lipid NPs	Non-covalent electrostatic interactions or hydrophobic interactions	≤70%	[11]

observed from 41% after 2 h to 94% after 16 h. The release is due to the protonation of the carboxylate groups and the formation of neutral BODIPY species, decreasing the interactions between BODIPY and the PMINPs matrix and therefore resulting in a release of BODIPY.

To monitor the delivery of BODIPY in cells, we incubated PMINPs and PMINPs@BODIPY with MDA-MB-231 breast cancer cells for 24 h at a concentration of 20 $\mu g.mL^{-1}$. Cells were also treated with BODIPY alone, as a control, at a concentration of 13 $\mu g.mL^{-1}$. Confocal Microscopy imaging confirmed the successful delivery of BODIPY and its diffusion from PMINPs to the cytoplasm of the cells as shown in Figure 7. It was not possible to visualize free BODIPY molecules inside the cells due to their inability to cross cell membranes. This result confirms the effectiveness of PMINPs as drug carrier.

We then addressed the binding ability of PMINPs@BODIPY towards siRNA. As already reported, PMINPs efficiently bind siRNA *via* ionic interactions.[5] Here, we studied if BODIPY loaded PMINPs still display the ability to adsorb siRNA. For this purpose,

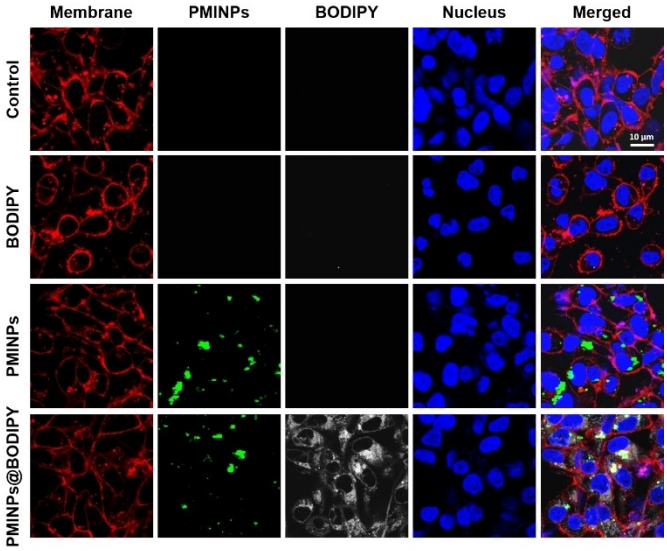

Figure 7. Confocal microscopy images of living MDA-MB-231 breast cancer cells treated with BODIPY, PMINPs or PMINPs@BODIPY. Cell membrane, PMINPs, BODIPY and nucleus appear in red, green, white, and blue colours, respectively.

we preformed agarose gel electrophoresis 2% (w/v) with various PMINPs@BODIPY/siRNA ratios (Figure 8).

These tests were carried out by adding a fixed amount of siRNA to increasing amounts of either free PMINPs or PMINPs@BODIPY with weight ratios ranging from 1/3 to 1/30. The mixtures were incubated for 30 min at 37 °C, and then electrophoresed.

Complexation of siRNA with free PMINPs showed complete siRNA adsorption in all tested weight ratios, ranging from 1/3 to 1/30, as previously reported (Figure 8a).[5] Slight differences could be observed using PMINPs@BODIPY (Figure 8b). Incomplete complexation of siRNA was observed for the ratio of 1/3, as indicated by the presence of the characteristic siRNA spot. In contrast, nearly complete siRNA complexation could be observed at the ratio 1/5, and total siRNA complexation was observed for the ratios 1/7, 1/10, 1/20 and 1/30. We can therefore notice a slightly decreased adsorption capacity of the PMINPs@BODIPY nanoparticles for the adsorption of siRNA compared to free PMINPs. This difference might be due to a partial occupation of the cationic adsorption sites located at the surface of the nanoparticles as also indicated by the slight decrease of the zeta potential values of BODIPY loaded nanoparticles PMINPs@BODIPY compared to unloaded PMINPs. Nevertheless, this decrease has no impact as long as we always use the ratio 1/10 for *in vitro* studies.

After having successfully established the complexation of siRNA with PMINPs@BODIPY, we investigated the photobiological activity of PMINPs@BODIPY on MDA-MB-231 breast cancer cells, which was compared to PMINPs activity, with or without green light exposure at 545 nm for 15 min (34 $J.cm^{-2}$).

Figure 9a displays a similar photodynamic effect between PMINPs and PMINPs@BODIPY at 10 $\mu g.mL^{-1}$ after green light irradiation, with cell death rates of 7 ± 1.4% and 3 ± 3.0% for cells treated with PMINPs and PMINPs@BODIPY, respectively. This experiment confirms that BODIPY loading conserves the phototoxic activity of PMINPs.

We investigated also the biological activity of the siRNA/PMINPs@BODIPY complex in plated MDA-MB-231-LUC-RFP cells, using siRNA molecules targeted against luciferase gene (siFluc), with or without green light irradiation at 545 nm for 5 min (11.3 $J.cm^{-2}$).

Figure 9b shows that free siFluc does not significantly decrease the luciferase activity when incubated with cells,

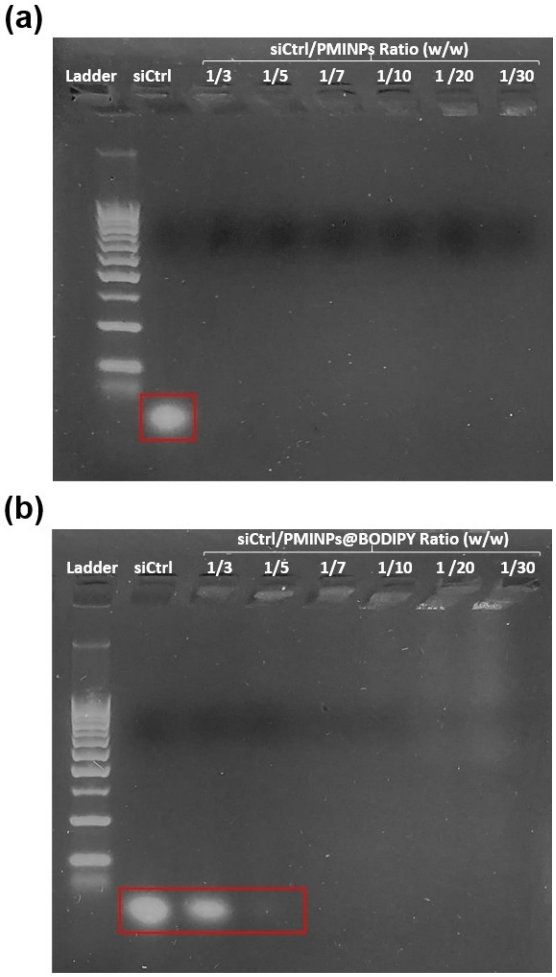

Figure 8. siRNA complexation study with free PMINPs and PMINPs@BODIPY. Agarose gel retardation assay for (a) PMINPs and (b) PMINPs@BODIPY complexed with siRNA negative control (siCtrl) at different weight ratios ranging from 1/3 to 1/30. Electrophoresis was immediately performed after complex formation for 30 min at 37 °C.

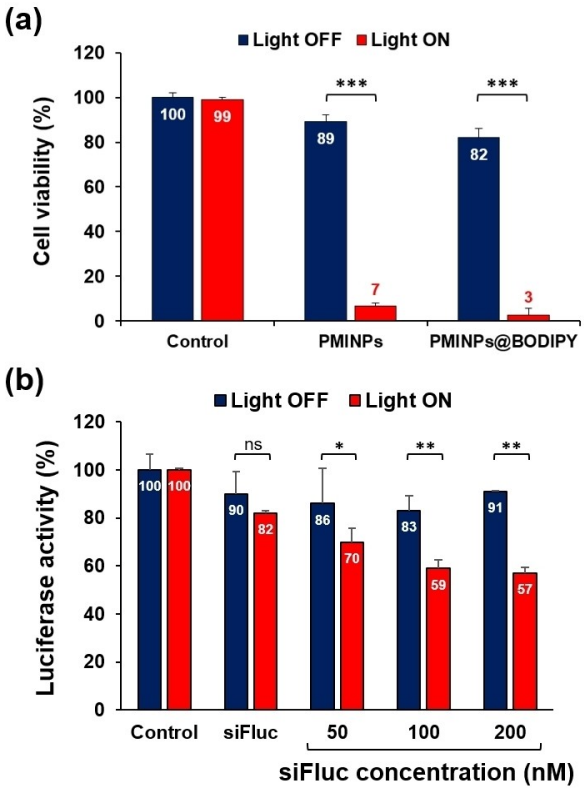

Figure 9. Evaluation of the biological activity of PMINPs@BODIPY *in vitro*. (a) Study of the photodynamic activity on MDA-MB-231 treated cells with PMINPs or PMINPs@BODIPY at 10 μg.mL^{-1} and irradiated (red bars) or not (blue bars) using green light (545 nm for 15 min, 34 J.cm^{-2}). (b) Study of gene silencing activity on MDA-MB-231 cells expressing luciferase and exposed (red bars) or not (blue bars) to light irradiation (545 nm for 5 min, 11.3 J.cm^{-2}) by the measurement of luminescence related to luciferase activity. Cells were untreated (control) or treated with free-siFluc (100 nM) or siFluc/PMINPs@BODIPY with increasing concentration of siFluc (50, 100 and 200 nM). For both conditions, luciferase activity was measured after 48 h of treatment and cell viability was estimated by MTT assay to consider only luciferase expression by living cells. The results are presented as mean ± SD, ns is non-statistically significant, *, ** and *** statistically significant difference ($p < 0.05$, $p < 0.005$ and $p < 0.0005$ respectively).

neither with (18 ± 1.1 %) nor without light irradiation (10 ± 9.2 %). This result confirms the inability of free siRNA to penetrate into the cells. When the cells were treated with siFluc/PMINPs@BODIPY using increasing concentrations of siFluc (50 to 200 nM) and without light irradiation, no significant decrease of luciferase expression has been observed neither, as only 9 ± 0.4 % of luciferase activity is inhibited, even at high concentration of siFluc (200 nM). In contrast, under similar conditions and with green light irradiation a significant inhibition of luciferase activity of 30 ± 5.6 %, 41 ± 3.4 % and 43 ± 2.3 % for 50, 100 and 200 nM of siFluc, respectively, was observed. This result is due to the PCI mechanism, which triggers the disruption of the endo-lysosomal membranes and releases siRNA molecules into the cytosol of cells, thus resulting in a significant decrease of luciferase expression combined with efficient drug delivery as indicated by BODIPY release at slightly acidic pH.

Conclusion

In this work, we have successfully demonstrated the use of PMINPs as a multifunctional platform giving the dual ability to perform gene therapy by siRNA transport as well as the delivery of small hydrophobic molecules such as chemotherapeutic agents, in order to fight efficiently against cancer. The siRNA controlled delivery is triggered by the use of light excitation. On the other side, anionic chemotherapeutic molecules can be delivered *via* a pH-responsive mechanism. No release is observed at physiological pH (pH 7.4), whereas at acidic tumor microenvironment pH (pH around 4–5), a massive cargo release is attested.

Experimental Section

Materials

1,3,5,7-tetramethyl-2,6-diethyl-8-(4-carboxyphenyl)BODIPY was purchased from PorphyChem. All siRNA used were purchased from Eurogentec (Seraing, Belgium). The Firefly Luciferase siRNA (siFluc) targeting sequence (sense: 5′-CUUACGCUGAGUACUUCGAdTdT-3′ and anti-sense: 5′-UCGAAGUACUCAGCGUAAGdTdT-3′) and the control siRNA (siCtrl) without any biological activity (sense: 5′-CGUACGCGGAAUACUUCGAdTdT-3′ and anti-sense: 5′-UCGAAGUAUUCCGCGUACGdTdT-3′).

PMINPs' Synthesis

The nanoparticles were synthesized according to our previous publication.[5]

Transmission electron microscopy (TEM)

TEM observations were carried out using JEOL 1400 Plus instrument (120 kV). Samples were deposited from ethanolic suspensions (200 μg.mL^{-1}) onto a carbon-coated copper grid and were dried in air.

Scanning electron microscopy (SEM)

SEM was performed using a HITACHI S4800 (FEG-HR) apparatus (30 kV). PMINPs suspension was prepared in water at a concentration of 200 μg.mL^{-1}.

BODIPY Loading

The BODIPY loading in PMINPs was carried out in water at two different pH conditions [pH 7 (phosphate buffer) and pH 8.5 (ammonium buffer)] using increasing feed weight ratios (fwr – Equation 1) ranging from 30 to 100% of BODIPY, for a fixed amount of PMINPs.

$$fwr\ (\%) = \frac{Mass\ of\ BODIPY\ fed}{Mass\ of\ PMINPs}\ \text{X}\ 100 \quad (1)$$

The solutions of BODIPY at various concentrations were prepared. Then, 500 μL of each solution was mixed with 500 μL of PMINPs suspension at 1 mg/mL to reach different fwr. The BODIPY loading into PMINPs was performed by simple soaking of BODIPY with PMINPs suspension. The soaking was achieved in dark condition, at room temperature and under stirring for 24 hours. The supernatants were then collected by centrifugation (20 000 rpm for 15 min), and analyzed by UV-Vis spectroscopy and absorbance measurements at 524 nm. The amounts of BODIPY loaded were calculated from calibration curves obtained with BODIPY solutions at various concentrations. UV-vis absorption spectra were collected at 25 °C on a JASCO V-750 spectrophotometer (France) using 10 mm quartz cells.

Two key parameters have been used in literature to evaluate the drug loading capacity of nanomedicines.[12] First, Drug Loading Content (DLC – Equation 2) is determined by the physico-chemical properties of the nano-system and represents the weight ratio of BODIPY loaded to PMINPs used. Second, Drug Loading Efficiency (DLE – Equation 3) is related to the used mass of drug in feed and the drug loading mechanism, and corresponds to the mass ratio percentage of BODIPY loaded to the amount of BODIPY initially introduced.

$$DLC\ (\%) = \frac{Mass\ of\ BODIPY\ loaded}{Mass\ of\ PMINPs}\ \text{X}\ 100 \quad (2)$$

$$DLE\ (\%) = \frac{Mass\ of\ BODIPY\ loaded}{Mass\ of\ BODIPY\ in\ feed}\ \text{X}\ 100 \quad (3)$$

BODIPY Release

The BODIPY release from PMINPs was performed in aqueous conditions supplemented with 10% of Dimethyl sulfoxide (DMSO) at pH 4 (acetate buffer) and pH 7.4 (PBS) for only fwr = 100%. The process was carried out in dark condition, at room temperature and without stirring.

The centrifugation pellets obtained at the end of the loading procedure were dispersed in 1 mL of buffer and BODIPY release was monitored by UV-Vis spectrophotometer absorbance at 524 nm, at different time points until 24 hours. The amounts of BODIPY released were calculated from calibration curves obtained with BODIPY solutions at various concentrations.

Getting good drug loading skills is not a sufficient parameter for a nanomedicine to be considered as a good carrier for drug delivery. PMINPs should be able to release a maximum amount of BODIPY loaded from their porosities. That is why a third key parameter must be added to evaluate drug delivery abilities of nanoparticles. Drug Released (DR – Equation 4) refers to mass ratio between BODIPY released and BODIPY loaded.

$$DR\ (\%) = \frac{Mass\ of\ BODIPY\ released}{Mass\ of\ BODIPY\ loaded}\ \text{X}\ 100 \quad (4)$$

Fluorescence Spectroscopy

Emission spectra were recorded at 25 °C on a fluorescence spectrophotometer (FS920, Edinburgh Instruments) with a 450 W continuous Xenon arc lamp using a quartz cuvette with 1.0 cm excitation path length and an aqueous solution of PMINPs or PMINPs@BODIPY at 200 μg.mL^{-1}. Excitation wavelength was 430 nm.

Cell lines

Human breast cancer cell line (MDA-MB-231) was purchased from ATCC. MDA-MB-231-LUC-RFP stable cell line was obtained from AMSBIO (SC041, Abingdon, UK). Cells were grown in Dulbecco's Modified Eagle Medium Gibco™ (DMEM) supplemented with 10% fetal bovine serum (FBS) and 1% gentamycin 100 μg.mL^{-1}. All cells were incubated at 37 °C in humidified atmosphere with 5% CO_2.

Imaging

MDA-MB-231 cells were seeded into glass bottom 8-well tissue culture chambers (SARSTEDT, Germany), at a density of 10^6 cells cm^{-2} for 24 hours. Then, cells were incubated for 24 hours with 500 μL culture medium containing 20 μg.mL^{-1} PMINPs, PMINPs@BODIPY or 13 μg.mL^{-1} BODIPY (which corresponds to BODIPY amount contained in PMINPs@BODIPY). Untreated cells

were considered as a negative control. 20 min prior the end of incubation, cells were loaded with CellMask™ Orange plasma membrane stain (Invitrogen, France) and Hoechst 33342 nucleus stain (Invitrogen, USA) at a final concentration of 5 $\mu g.mL^{-1}$ and 10 $\mu g.mL^{-1}$, respectively. Then, cells were washed three times with culture medium before observation with LSM780 confocal microscope (Carl Zeiss, Germany). Cells were scanned at 780 nm for PMINPs, 488 nm for BODIPY, 561 nm for CellMask and 760 nm for Hoechst, using a high magnification (63x/1.4 OIL Plan-Apo).

Agarose gel retardation assay

A fixed quantity (0.364 μg) of siCtrl was added to increasing amounts of PMINPs or PMINPs@BODIPY, in order to obtain increasing weight ratios (from 1/3 to 1/30). The mixtures were incubated at 37 °C for 30 min. After incubation, siCtrl/PMINPs and siCtrl/PMINPs@BODIPY complexes were mixed with xylene cyanol 0.25 % then electrophoresed on 2 % (w/v) agarose gel containing GelRed™ Nucleic Acid Gel Stain (Interchim, France), with running buffer Tris–Borate–EDTA (TBE) 0.5X, pH 8.2 at 100 V for 30 min. siCtrl bands were visualized and photographed by an ultraviolet transilluminator (Infinity Gel Documentation Imaging, Vilber Lourmat, France).

Photodynamic effect experiment

MDA-MB-231 cells were seeded in 96-well plate at a density of 3000 cells *per* well in their respective medium. Twenty-four hours after, cells were treated with PMINPs or PMINPs@BODIPY at a concentration of 10 $\mu g.mL^{-1}$ then were left to incubate for 24 h. Control cells were treated with the vehicle only. After the end of the incubation period, cells were irradiated (or not) with a green light beam at 545 nm for 15 min (34 $J.cm^{-2}$), using a microscope objective lens (4X/0.10). 48 h later, the phototoxic effect of nanoparticles was evaluated by cell viability measurements using the colorimetric assay 3-(4,5-dimethylthiazol-2-yl)-2,5-diphenyltetrazolium bromide (MTT), in which cells were incubated with 0.5 $mg.mL^{-1}$ of MTT for 4 h, followed by aspiration of the medium, addition of the mixture of ethanol/DMSO (1/1, v/v), shaking for 20 min and absorbance reading at 540 nm. The cell viability percentage (%) was calculated according to the non-irradiated control (set as 100 %).

Luciferase gene silencing by siFluc delivery

24 hours prior to transfection, MDA-MB-231-LUC-RFP cells were plated at a density of 3000 cells *per* well, into 96-well white plate, PS, F-bottom, μCLEAR® (Greiner bio-one, Germany). siFluc/PMINPs@-BODIPY were freshly prepared in serum free cell culture medium for 30 min at 37 °C using different concentrations of siFluc (50, 100 and 200 nM) at a weight ratio of 1/10. Then, cells were treated (or not) with siFluc/PMINPs@BODIPY complexes for 4 hours. After that, FBS was added in each well to reach a 10 % serum. After 8 hours of incubation, cells were submitted to light irradiation at 545 nm for 5 min duration (11.3 $J.cm^{-2}$). The light beam was focused by a microscope objective lens (4x/0.10). After 48 hours of transfection, luciferase activity was evaluated by addition of D-Luciferin (PerkinElmer, USA) at a final concentration of 10^{-3} M. Cell luminescence was measured 10 min after, with a plate reader CLARIOstar high performance monochromator multimode microplate reader (BMG Labtech, Ortenberg, Germany). Results are expressed as a percentage of luminescence activity of treated cells compared to the control cells (set as 100 %). Luciferase activity was corrected according to the total number of living cells in each well, as determined by the MTT assay.

Statistical analysis

Results were presented as mean ± standard deviation (SD) of three independent experiments. The comparison between groups was analyzed with Student's t-test. Differences were considered statistically significant when p values were less than 0.05. The level of significance was defined as ns (non-statistically significant), * statistical significance difference ($p < 0.05$), ** ($p < 0.005$) and *** ($p < 0.0005$).

Acknowledgements

The authors thank the "Algerian Ministry of Higher Education and Scientific Research" for the Ph.D. grant to B.M. and the Franco-Algerian steering committee for its support. We also thank Montpellier RIO Imaging platform (ANR-10-INBS-04), member of FranceBioImaging, for imaging facilities.

Conflict of Interest

The authors declare no conflict of interest.

Data Availability Statement

The data that support the findings of this study are available from the corresponding author upon reasonable request.

Keywords: BODIPY · drug delivery · periodic mesoporous ionosilica nanoparticles · photochemical internalization · siRNA

[1] a) R. S. Guimarães, C. F. Rodrigues, A. F. Moreira, I. J. Correia, *Pharmacol. Res.* **2020**, *155*, 104742; b) Y. Cheng, X. Jiao, W. Fan, Z. Yang, Y. Wen, X. Chen, *Biomaterials* **2020**, *256*, 120191; c) Z. Teng, W. Li, Y. Tang, A. Elzatahry, G. Lu, D. Zhao, *Adv. Mater.* **2018**, *0*, 1707612; d) X. Du, F. Kleitz, X. Li, H. Huang, X. Zhang, S.-Z. Qiao, *Adv. Funct. Mater.* **2018**, *28*, 1707325; e) X. Du, X. Li, L. Xiong, X. Zhang, F. Kleitz, S. Z. Qiao, *Biomaterials* **2016**, *91*, 90–127; f) Y. Chen, J. Shi, *Adv. Mater.* **2016**, *28*, 3235–3272; g) J. G. Croissant, X. Cattoen, M. Wong Chi Man, J.-O. Durand, N. M. Khashab, *Nanoscale* **2015**, *7*, 20318–20334; h) C. Xu, C. Lei, Y. Wang, C. Yu, *Angew. Chem. Int. Ed.* **2022**, *61*, e202112752; i) N. X. D. Mai, T.-H. T. Nguyen, L. B. Vong, M.-H. D. Dang, T. T. T. Nguyen, L. H. T. Nguyen, H. K. T. Ta, T.-H. Nguyen, T. B. Phan, T. L. H. Doan, *Mater. Sci. Eng. C* **2021**, *127*, 112232; j) L. Guan, J. Chen, Z. Tian, M. Zhu, Y. Bian, Y. Zhu, *VIEW* **2021**, *2*, 20200117.

[2] R. Bouchal, M. Daurat, M. Gary-Bobo, A. Da Silva, L. Lesaffre, D. Aggad, A. Godefroy, P. Dieudonné, C. Charnay, J.-O. Durand, P. Hesemann, *ACS Appl. Mater. Interfaces* **2017**, *9*, 32018–32025.

[3] A. D. Rodrigues, M. Jacob, V. Gauchou, J. O. Durand, P. Trens, B. Prelot, P. Hesemann, *Microporous Mesoporous Mater.* **2021**, *310*, 110644.

[4] M. Daurat, S. Rahmani, R. Bouchal, A. Akrout, J. Budimir, C. Nguyen, C. Charnay, Y. Guari, S. Richeter, L. Raehm, N. Bettache, M. Gary-Bobo, J.-O. Durand, P. Hesemann, *ChemNanoMat* **2019**, *5*, 888–896.

[5] B. Mezghrani, L. M. A. Ali, S. Richeter, J.-O. Durand, P. Hesemann, N. Bettache, *ACS Appl. Mater. Interfaces* **2021**, *13*, 29325–29339.

[6] a) D. Tarn, C. E. Ashley, M. Xue, E. C. Carnes, J. I. Zink, C. J. Brinker, *Acc. Chem. Res.* **2013**, *46*, 792–801; b) Slowing, II, J. L. Vivero-Escoto, C. W. Wu, V. S. Y. Lin, *Adv. Drug Delivery Rev.* **2008**, *60*, 1278–1288.

[7] a) J. L. Gu, S. S. Su, Y. S. Li, Q. J. He, J. L. Shi, *Chem. Commun.* **2011**, *47*, 2101–2103; b) L. Zhou, K. Dong, Z. W. Chen, J. S. Ren, X. G. Qu, *Carbon* **2015**, *82*, 479–488; c) H. Wang, X. G. Li, Z. Q. Ma, D. Wang, L. Z. Wang, J. Q. Zhan, L. She, F. Yang, *Int. J. Nanomed.* **2016**, *11*, 1793–1806.

[8] a) W. Cai, C. C. Chu, G. Liu, Y. X. J. Wang, *Small* **2015**, *11*, 4806–4822; b) M. Wu, Q. T. Wang, X. L. Liu, J. F. Liu, *RSC Adv.* **2015**, *5*, 30970–30980; c) L. M. A. Ali, E. Mathlouthi, M. Cahu, S. Sene, M. Daurat, J. Long, Y. Guari, F. Salles, J. Chopineau, J. M. Devoisselle, J. Larionova, M. Gary-Bobo, *RSC Adv.* **2020**, *10*, 2646–2649.
[9] a) D. M. Ren, F. Kratz, S. W. Wang, *Small* **2011**, *7*, 1051–1060; b) D. M. Ren, M. Dalmau, A. Randall, M. M. Shindel, P. Baldi, S. W. Wang, *Adv. Funct. Mater.* **2012**, *22*, 3170–3180; c) A. Jain, S. K. Singh, S. K. Arya, S. C. Kundu, S. Kapoor, *ACS Biomater. Sci. Eng.* **2018**, *4*, 3939–3961.
[10] a) J. W. Guo, X. L. Gao, L. N. Su, H. M. Xia, G. Z. Gu, Z. Q. Pang, X. G. Jiang, L. Yao, J. Chen, H. Z. Chen, *Biomaterials* **2011**, *32*, 8010–8020; b) Y. Malinovskaya, P. Melnikov, V. Baklaushev, A. Gabashvili, N. Osipova, S. Mantrov, Y. Ermolenko, O. Maksimenko, M. Gorshkova, V. Balabanyan, J. Kreuter, S. Gelperina, *Int. J. Pharm.* **2017**, *524*, 77–90; c) N. Ahmad, R. Ahmad, M. A. Alam, F. J. Ahmad, *Chem. Cent. J.* **2018**, *12*.
[11] a) D. Poy, H. E. Shahemabadi, A. Akbarzadeh, H. Moradi-Sardareh, M. Ebrahimifar, *Int. J. Polym. Mater. Po.* **2018**, *67*, 367–370; b) M. S. Franco, M. C. Roque, M. C. Oliveira, *Pharmaceutica* **2019**, *11*; c) M. Fu, W. Tang, J. J. Liu, X. Q. Gong, L. Kong, X. M. Yao, M. Jing, F. Y. Cai, X. T. Li, R. J. Ju, *J. Drug Targeting* **2020**, *28*, 245–258.
[12] a) M. Menard, F. Meyer, K. Parkhomenko, C. Leuvrey, G. Francius, S. Begin-Colin, D. Mertz, *BBA-Gen. Subjects* **2019**, *1863*, 332–341; b) S. H. Shen, Y. S. Wu, Y. C. Liu, D. C. Wu, *Int. J. Nanomed.* **2017**, *12*, 4085–4109.

Manuscript received: January 12, 2023
Revised manuscript received: February 10, 2023
Accepted manuscript online: February 13, 2023